Macromol. Symp. **2007**, 249–250, 251–258 DOI: 10.1002/masy.200750341

Synthesis and Characterization of Waterborne Polyurethane/Clay Nanocomposite – Effect on Adhesive Strength

*Mohammad Mizanur Rahman, Hye-Jin Yoo, Chung Jung Mi, Han-Do Kim**

Summary: Waterborne polyurethane (WBPU)/clay nanocomposites were synthesized using prepolymer process with different clay content (0–5 wt%) of organoclay cloisite 15A. The optimum dispersion temperature of clay in polyol was found to be 80 °C at 3 hours. The XRD confirmed the exfoliation dispersion of clay by polyol in WBPU/clay nanocomposite. IR and ^{1}H-NMR spectroscopy confirmed the unreacted condition of clay component. Particle size of the WBPU/clay nanocomposite dispersion was increased with increasing of clay concentration. Water swelling was decreased with increasing of clay up to the optimum content (2 wt %) and then leveled off. The thermal stability, mechanical property and adhesive strength were increased with increasing clay content up to 2 wt% to reach its maximum value.

Keywords: adhesion; clay; nanocomposites; polyurethanes; waterborne

Introduction

Polymer/clay nanocomposites have attracted much more attention in the recent decades[1] because of their unique properties compared with those of the conventional composites. Among those properties are higher strength and modulus,[1,2] better dimensional and thermal stabilities,[3,4] as well as improved barrier properties and chemical stability.[4,5] Polymer/clay nanocomposites can be generally classified into two groups. The intercalated polymer/clay nanocomposites have layered clay dispersed in a polymer matrix with polymer chains inserted into clay layers that retain their lateral order. The exfoliated ones consist of fully delaminated clay platelets dispersed individually in the matrix. Thus, each platelet interacts with the matrix and improves the properties of the nanocomposites more effectively.

Environmental friendly waterborne polyurethane (WBPU) has been rapidly used in coating and adhesive from last two decades.[6–11] However, the WBPU is deficient in chemical resistance, thermal resistance, and mechanical property compared to solvent based polyurethane. Methods have been employed to improve these disadvantages of WBPU such as hydrophobic monomers grafted to PU main chain,[12,13] the change of the type and content of ionic center,[14–16] the adjustment of ionic neutralization degree[17–19], the blend[20–22] and copolymerization[23–27] of different polymers, and cross-linking.[28,29]

Recently, the polyurethane clay nanocomposite is attracted much more due to significant improvement of thermal, and mechanical properties of clay composite materials.[30–32] However, very little research has been done in WBPU/clay nanocomposite.[33,34] Moreover there is no proper information about the synthesis of WBPU/clay nanocomposite, more precisely the experimental parameter such as mixing time and temperature and clay concentration.

In this study, we synthesized WBPU/clay nanocomposite using prepolymer process at various clay content (0–5 wt%) using organoclay cloisite 15A. We investigated

---

Department of Textile Engineering, Pusan National University, Busan, Korea

the reactivity of clay and structure such as intercalated or exfoliated structure of WBPU/clay nanocomposite. We conduct our research on effect of clay content on particle size of the dispersion, water swelling, thermal stability and mechanical properties of the films. Our study also evaluates the adhesive strength of WBPU/clay nanocomposite with respect of different clay content.

Experimental Part

Materials

Poly tetramethylene adipate glycol (PTAd, number-average molecular weight = 2000 g/mol; Aldrich Chemical) was dried at 90 °C and 1–2 mmHg for 3 h before use. Dimethylol propionic acid (DMPA, Aldrich Chemical, Milwaukee, WI), Tri-ethyl amine (TEA; Junsei Chemical, Tokyo, Japan), *N*-methyl-2-pyrrolidone (NMP; Junsei Chemical), 4,4-dicyclohexylmethane diisocyanate (H_{12}MDI, Aldrich Chemical), and ethylene diamine (EDA, Junsei Chemical) were used after dehydration with 4-Å molecular sieves for 1 week. Dibutyltin dilaurate (Aldrich Chemical), a thickener (L75N, Bayer, Leverkusen, Germany), and hardener (ARF 30), were used without further purification. The clay, Cloisite® 15A containing 90 mequiv./100 g clay of quaternary ammonium ions, was kindly donated by Southern Clay Products (Gonzales, TX, USA). The quaternary ammonium ion has a structure, $N^+(CH_3)_2$-$(HT)_2$, with HT representing an hydrogenated tallow of approximately 65% $C_{18}H_{37}$, 30% $C_{16}H_{33}$, and 5% $C_{14}H_{29}$.[35]

Synthesis of the WBPU/Clay Nanocomposite Dispersions

The WBPU/clay nanocomposites were synthesized with the prepolymer mixing process. PTAd was placed in a four-necked separable flask equipped with a thermometer, a stirrer, a condenser with a drying tube, an inlet of dry nitrogen, and a heat jacket and was degassed in vacuum at 85 °C for 30 min. Clay was added to the polyol and stirred at 80 °C for swelling of clay in polyol. After 3 hours, the clay was exfoliated by polyol which was confirmed by XRD. DMPA/NMP (1/1 w/w) was added to the flask, and the mixture was allowed to cool to 40 °C under moderate stirring (175 ~ 200 rpm). Then, H_{12}MDI was added to the flask, and the mixture was heated to 85 °C under moderate stirring (175 ~ 200 rpm). The reaction mixture was allowed to react at 85 °C until the theoretical NCO content was reached. The change in the NCO value during the reaction was determined with the standard dibutylamine back-titration method (ASTM D 1638). Then, methyl ethyl ketone (MEK; 20 wt%) was added to the NCO-terminated prepolymer mixture to adjust the viscosity of the solution. TEA was added to the reaction mixture to neutralize the carboxyl group of the NCO-terminated polyurethane prepolymer. After 30 min of neutralization, distilled water (60 wt%) was added to the reaction mixture with vigorous stirring (1300 ~ 1500 rpm). The dispersion was chain-extended by the dropping of EDA at 40 °C for 1 h, and the reaction continued until the NCO peak (2270 cm^{-1}) in the IR spectra had completely disappeared. All of the WBPU/clay nanocomposite (30 wt% solid content) were obtained by the evaporation of MEK and the subsequent addition of an adequate amount of distilled water.

Preparation of the WBPU/Clay Nanocomposite Films

The WBPU/clay nanocomposite films were prepared by pouring the aqueous dispersion on a Teflon disk under the ambient conditions for 48 hours. The films (typically about 0.5 mm thick) were dried in vacuum at 50 °C for 1 day and stored in a desiccator at room temperature. The adhered materials were formulated using synthesized WBPU/clay nanocomposite dispersion, a thickener (L75N, 0.5 wt%), and a hardener (ARF 30, 5.0 wt%). The adhered material was coated on the nylon fabrics and another nylon fabrics was laid on the coated surface and then dried at 100 °C under fixed pressing condition (15 kgf/cm^2) for 10 minutes.

Characterization

The X-ray diffraction (XRD) patterns were recorded using a Philips Xpert XRD System diffractometer at a voltage of 40 kV, of current and a radiation of wavelength 1.542 Å. Diffraction patterns were obtained in the range of Bragg's angle $2\theta = 0°–40°$. The 2θ scan rate was 2 °C/min.

The scanning electron microscopy (SEM) micrographs of WBPU/clay nanocomposite were obtained with a Hitachi (Japan) S-4200 field emission scanning electron microscope at 5 kV.

The mean particle size of the WBPU/clay nanocomposite was measured using laser-scattering equipment (Autosizer, Melvern IIC, Malvern, Worcester, UK). A small amount of dispersion was added in a deionised water tank and this was followed by the pinhole being set at 200 μm. The average particle diameters were measured at 25 °C.

A Fourier transform infrared spectrometer (Impact 400D, Nicolet, Madison, WI) was used to identify the WBPU/clay nanocomposite structure. For each IR spectrometer sample, 32 scans at a 4-cm^{-1} resolution were collected in the transmittance mode.

^{1}H-NMR spectra of the WBPU/clay nanocomposite was recorded in a Fourier transform Bruker 300 MHz spectrometer model AC-300. 30 mg of the film was dissolved in 4 ml of deuterated chloroform. TMS was used as an internal reference.

Water swelling of the WBPU/clay nanocomposite films was determined by immersing the films in water at 25 °C. Three parallel measurements were carried out for each sample. The water swelling of the films was calculated by

$$\text{Swelling}\,(\%) = \frac{W - W_0}{W_0} \times 100$$

Where W_0 is the weight of the dried film and W is the weight of the film at equilibrium swelling.

Thermal gravimetry analysis was performed in a Pyris 6 TGA (Perkim Elmer, USA). 5.0 mg of the films were placed in a platinum pan and heated from 30 to 500 °C under N_2, at a heating rate of 10 °C/min.

The tensile properties were measured at room temperature with a United Data System tension meter (SSTM-1 United Data Systems, Instrom, Japan) according to the ASTM D 638 specifications. A crosshead speed of 30 mm/min was used throughout these investigations to determine the ultimate tensile strength and modulus and the elongation at break for all the samples. The values quoted are the average of five measurements. The adhesion property was measured with the United Data System tension meter according to the ASTM D 1876-01(the peel resistance of adhesives, i.e., the T-peel test). The values obtained were the average of five measurements (standard deviation was less than 5%).

Result and Discussion

The sample designations and compositions of WBPU/clay nanocomposite is shown in Table 1. We synthesized WBPU/clay nanocomposite of various clay concentration

Table 1.
Sample designation and composition of WBPU/clay nanocomposite.

Sample	Composition (molar ratio)					DMPA	Clay
Designation	PTAd	DMPA	$H_{12}MDI$	TEA	EDA	(wt%)	(wt%)
P0	0.040	0.054	0.112	0.054	0.018	6.16	0
P1							1
P2							2
P3							3
P4							4
P5							5

(0 ~ 5 wt%) at a fixed composition of soft segment and hard segment.

The effect of mixing temperature of clay in polyol was investigated. It was found that at a temperature of 30 °C no dispersion occurred. However, with increasing of mixing temperature, the peak intensity was decreased slowly and eventually disappeared at 80 °C and 100 °C. This result suggests that the mixing temperature is an important factor for clay dispersion in polyol and the optimum temperature was found 80 °C. Moreover, the dispersion behavior of clay in polyol with different time at a fixed temperature 80 °C was also conducted. It was found that with time passing the clay dispersion was increased and fully dispersed after 3 hour which was confirmed by disappearance of the peak. XRD analyses of WBPU/clay nanocomposites with different clay concentrations are shown in Figure 1. Each WBPU/clay nanocomposite exhibits a broad, amorphous diffraction halo at $2\theta = 19.26$, which is the same as that of pure WBPU. This diffraction halo is associated with the amorphous phase of WBPU. The characteristic peak of the clay cloisite 15A was found previously at $2\theta = 6.95$, disappears fully after WBPU/clay nanocomposite formation. Moreover, there is no diffraction peaks observed in the 2θ range of 0.5–6.95. This indicates that most clay platelets are exfoliated. For many solvent-based PU nanocomposites with the absence of ions in PU moieties, the electrostatic forces between the clay platelets have a tendency to squeeze the PU polymer chains out and subsequently result in an intercalated structure.[30–32,36–38] The clay intercalated with the PU polymer exhibits a reflection at $2\theta = 2.5$, for a certain solvent-based polyurethane nanocomposite.[36] In the WBPU/clay nanocomposite system studied in this work, the aforementioned squeeze effect has been overcome by the ionic attractions between anionic WBPUs and cationic clay platelets.

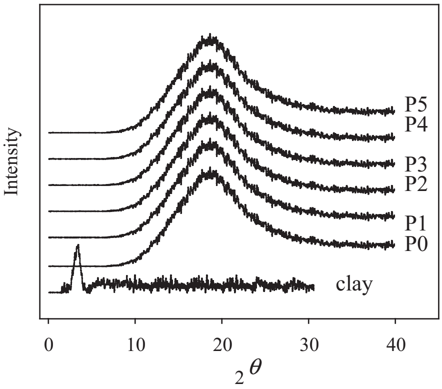

Figure 1.
XRD of WBPU/clay nanocomposite.

Therefore, the intercalated WBPU polymer chains can peel the platelets away from the well-intercalated silicate stacks or tactoids, and this result is an exfoliated silicate system. However, this is not possible to get idea of clay orientation such as homogeneous or heterogeneous in the WBPU/clay nanocomposite by XRD.

The WBPU/clay nanocomposite was further characterized by SEM, the image of which is shown in Figure 2 (as a representative sample). It is observed that the clay was dispersed well when clay content is less than 2 wt%. Excess clay (3 ~ 5wt%) was in aggregated state in the WBPU/clay nanocomposite. The aggregated condition of the clay was increased with increasing of clay content. However, clay platelets were randomly oriented in WBPU/clay nanocomposite.

The mean particle size of the WBPU/clay nanocomposite dispersion increased with increasing of clay content (Figure 3). Generally, the particle size of the WBPU dispersion is governed by the hydrophilicity of the ionomer.[39] The mean particle size was increased in the dispersion with increasing of hydrophobic clay content indicates the inclusion of clay particle in the dispersion.

The structure of the WBPU/clay nanocomposite was analyzed by FT-IR spectroscopy, as shown in Figure 4(a). In the spectra, it is very hard to find any new peak in WBPU/clay nanocomposite comparing with pure WBPU. This implies that the clay was unreacted state in WBPU/clay nanocomposite. However, all of the major

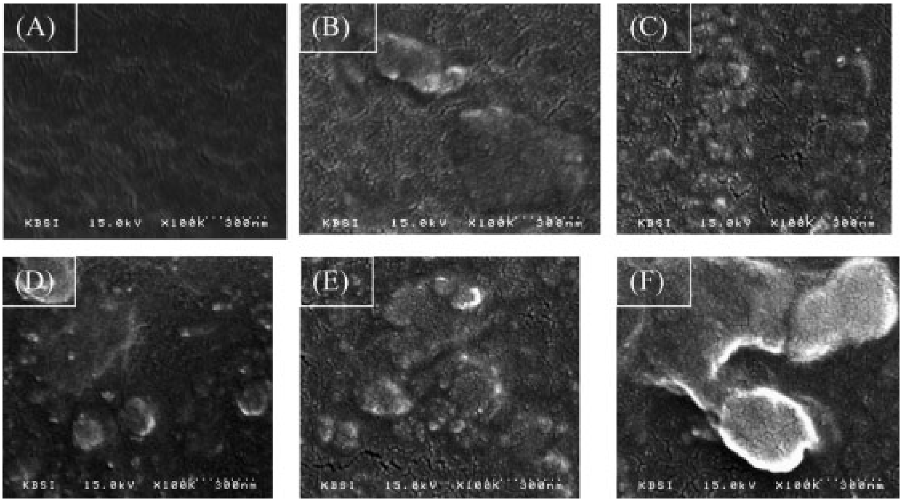

Figure 2.
SEM image (A) pure WBPU and WBPU/clay nanocomposite (B) clay 1 wt%, (C) clay 2 wt% (D) clay 3 wt% (E) clay 4 wt% (F) clay 5 wt%.

characteristic peaks of polyurethane were found in the WBPU/clay nanocomposite.

The ^{1}H-NMR spectroscopy provides more conclusive evidence for the structures of WBPU/clay nanocomposite. In Figure 4(b), the ^{1}H-NMR spectra of the WBPU/clay nanocomposite is shown. It was found that there were no major changes in the spectra.

This indicated that the clay couldn't participate any reaction; it just swelled by polyol and remains in the unreacted state. However, the NMR peaks of WBPU/clay nanocomposites become broadened with presence of clay. Since the NMR measurements were carried out in the solution state, this behavior implies that the mobility of polyurethane molecules in chloroform was restricted by the silicate layers of the clay.

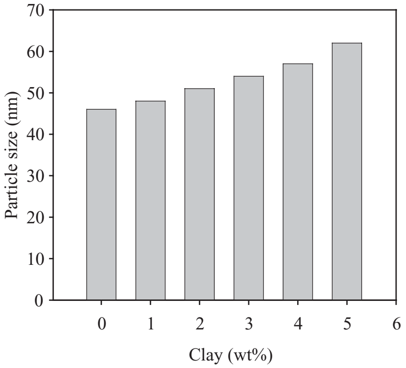

Figure 3.
Particle size of dispersion.

In Figure 5 the water swelling nature of the WBPU/clay nanocomposite film has been shown. It was found that the water swelling was decreased with increasing of clay up to the optimum content and then leveled off. Due to the nanaometer organoclay layer in WBPU/clay nanocomposite, the mean free path was decreased and resists water swelling.[40]

TGA is a good method to determine the thermal stability of the WBPU/clay nanocomposite film. The TGA curves for all samples indicate that there are two stages of decomposition (Figure 6). It indicates that the clay has no effect on decomposition stage of WBPU/clay nanocomposite. However, the decomposition temperature was increased definitely which implys of thermal stability of WBPU/clay nanocomposite. The increase of the thermal stability could be attributed to the high thermal stability of the clay and the interaction between the clay particles and the PU-urea matrix.[41] Since the chain motions of polymer molecules in these silicate layers were

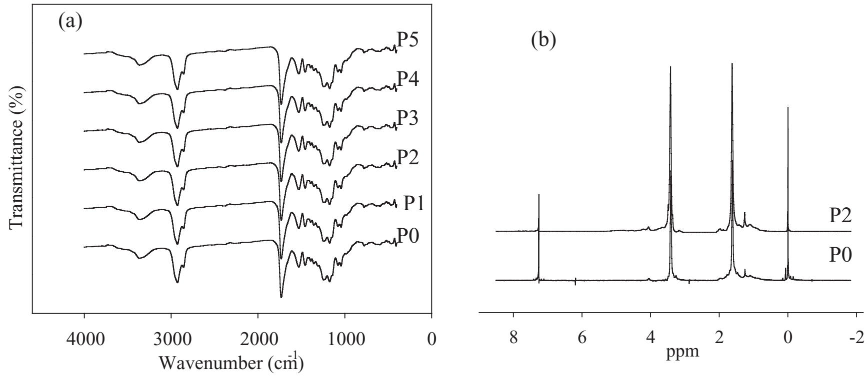

Figure 4.
IR spectra (a) and ^{1}HNMR spectra (b) of WBPU/clay nanocomposite.

barred and limited, therefore, thermal properties of the nanocomposites increased.[42] The other probable cause will be the layered silicates make the path longer for escaping of the thermally decomposed volatiles, or in other words clay particles can enhance the thermal stability of the polymer by acting as thermal insulator and mass transport barrier to the volatile products generated during decomposition. Similar trends have been noted in other articles also.[43–46]

To investigate the effect of clay content on mechanical properties of WBPU/clay nanocomposite, the stress-strain curves has been shown in Figure 7. It was found that the clay increase the mechanical properties up to the optimum content, then little decreased with excess of clay content. The increase of mechanical strength up to optimum content (2 wt%) due to good compatibility of nanometer clay layers and strong interaction with pure WBPU. However, the decrease of the mechanical strength of the WBPU/clay nanocomposite with more then 2 wt% may be due to the aggregation of excess clay.

Figure 8 shows the effect of clay content on adhesive strength of WBPU/clay nanocomposite. It was found that the breaking was not occurred on the interface of fabrics/adhesive layer but occurred in adhesive layer itself. This implies that the strength of solid WBPU/clay nanocomposite is more important factor than the attraction forces between fabric and adhesives. The adhesive

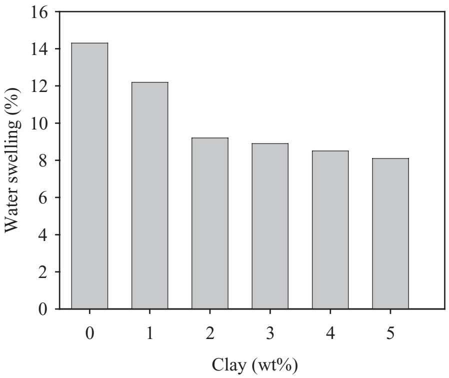

Figure 5.
Water swelling of the films.

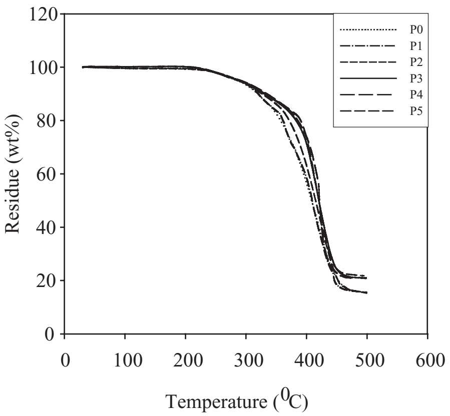

Figure 6.
TGA thermographs of the films.

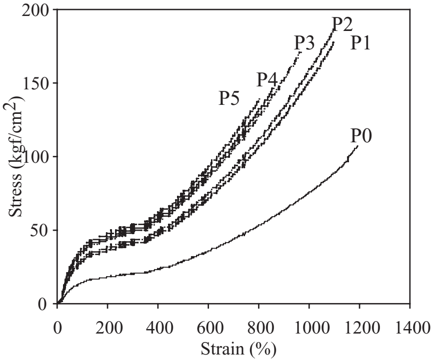

Figure 7.
Stress-strain curves of the films.

strength increased up to the optimum clay content (2 wt%) and then that of decreased with increased of clay content. May be this is due to the increase of mechanical property up to the optimum clay content which create more strong mechanical seal with the substrate nylon fabrics and increase the adhesive strength. However excess clay remained at aggregated state and decreased the adhesive strength.

Conclusion

WBPU/clay nanocomposite was successfully synthesized with different clay concentration (0 ~ 5wt%). It was confirmed by XRD that clay was exfoliated state in the WBPU/clay nanocomposite within 3h at 80 °C. The particle size of the WBPU/clay nanocomposite dispersion was increased with increasing clay concentartion. IR and NMR spectroscopy confirmed that the clay remain as unreacted state. Water swelling character decreased with increasing of clay content in the WBPU/clay nanocomposite. Thermal stability, mechanical strength and adhesive strength were maximum at 2 wt% clay concentration in WBPU/clay nanocomposite.

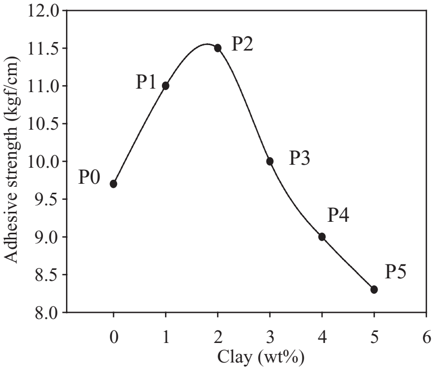

Figure 8.
Adhesive strength on nylon fabrics.

Acknowledgements: This work was performed through a program for cultivating graduate students in regional strategic industry.

[1] P. Messersmith, E. P. Giannelis, *Chem. Mater.* **1994**, *6*, 1719.
[2] T. Lan, T. J. Pinnavaia, *Chem. Mater.* **1994**, *6*, 2216.
[3] Z. Wang, T. J. Pinnavaia, *Chem. Mater.* **1998**, *10*, 1820.
[4] J. Massam, Z. Wang, T. J. Pinnavaia, T. Lan, G. Beall, *Polym. Mater. Sci. Eng.* **1998**, *78*, 274.
[5] J. Massam, T. J. Pinnavaia, *Mater. Res. Soc. Symp. Proc.* **1998**, *520*, 223.
[6] G. N. Chen, K. N. Chen, *J. Appl. Polym .Sci.* **1997**, *63*, 1609.
[7] D. Diterich, W. Keberie, H. Witt, *Angew Chem Int Ed Engl* **1970**, *9*, 40.
[8] F. M. B. Coutinho, M. C. Delpech, *Polym. Testing* **1996**, *15*, 103.
[9] M. C. Delpech, F. M. B. Coutinho, *Polym. Testing* **2000**, *19*, 939.
[10] C. H. Shao, J. J. Huang, G. N. Chen, J. T. Yeh, K. N. Chen, *Polym Degrad Stab.* **1999**, *65*, 359.
[11] F. M. B. Coutinho, M. C. Delpech, *Polym Degrad Stab.* **2000**, *70*, 49.
[12] D. K. Kim, S. B. Lee, K. S. Doh, Y. W. Nam, *J. Appl. Polym. Sci.* **1999**, *74*, 2029.
[13] J. W. Gooch, H. Dong, F. J. Schork, *J. Appl. Polym. Sci.* **2000**, *76*, 105.
[14] C. H. Lim, H. S. Choi, S. T. Noh, *J. Appl. Polym. Sci.* **2002**, *86*, 3322.
[15] S. Turri, M. Levi, T. Trombetta, *J. Appl. Polym. Sci.* **2004**, *93*, 136.
[16] C. K. Kim, B. K. Kim, *J. Appl. Polym. Sci.* **1991**, *43*, 2295.
[17] J. Y. Jang, Y. K. Jhon, I. W. Cheong, J. H. Kim, *Colloids Surf. A.* **2002**, *196*, 135.
[18] J. E. Yang, J. S. Kong, S. W. Park, D. J. Lee, H. D. Kim, *J. Appl. Polym. Sci.* **2002**, *86*, 2375.
[19] B. K. Kim, T. K. Kim, H. M. Jeong, *J. Appl. Polym. Sci.* **1994**, *62*, 371.
[20] M. Hirose, J. Zhou, K. Nagai, *Prog. Org. Coat.* **2000**, *38*, 27.

[21] T. Bremner, D. J. T. Hill, M. I. Killen, J. H. O'Donnell, P. J. Pomery, D. St. John, A. K. Whittaker, *J. Appl. Polym. Sci.* **1997**, *65*, 939.

[22] M. S. Yen, P. Y. Tsai, *J. Appl. Polym. Sci.* **2003**, *90*, 233.

[23] B. K. Kim, J. C. Lee, K. H. Lee, *J. Macromol. Sci. Pure Appl. Chem.* **1994**, *31*, 1241.

[24] H. Z. Zhuang, A. Camberlin, D. M. Hercules, *Macromolecules* **1997**, *30*, 1153.

[25] R. Adhikari, P. A. Gunatillake, S. J. McCarthy, G. F. Meijs, *J. Appl. Polym. Sci.* **1999**, *74*, 2979.

[26] B. K. Kim, J. C. Lee, *J. Polym. Sci. Part A: Polym. Chem.* **1996**, *34*, 1095.

[27] T. O. Ahn, S. U. Jung, H. M. Jeong, S. W. Lee, *J. Appl. Polym. Sci.* **1994**, *51*, 43.

[28] J. Y. Kwon, H. D. Kim, *Macromol.Rres*, **2006**, *14*, 373.

[29] K. Mequanint, R. Sanderson, *Polymer* **2003**, *44*, 2631.

[30] G. Gorrasi, M. Tortora, V. Vittoria, *J. Polym. Sci. Part B: Polym. Phys.* **2005**, *43*, 2454.

[31] J. H. Chang, Y. U. An, *J. Polym. Sci. Part B: Polym. Phys.* **2002**, *40*, 670.

[32] R. Xu, E. Manias, A. Snyder, J. Runt, *Macromolecules* **2001**, *34*, 337.

[33] B. K. Kim, J. W. Seo, H. M. Jeong, *European Polym. J.* **2003**, *39*, 85.

[34] H. C. Kuan, C. M. Ma, W. P. Chuang, H. Y. Su, *J. Polym. Sci. Part B: Polym. Phys* **2005**, *43*, 1.

[35] http://www.nanoclay.com/data/15A.htm.

[36] M. A. Osman, V. Mittal, M. Morbidelli, U. W. Suter, *Macromolecules* **2003**, *36*, 9851.

[37] B. Finnigan, K. Jack, K. Campbell, P. Halley, R. Truss, P. Casey, D. Cookson, S. King, D. Martin, *Macromolecules* **2005**, *38*, 7386.

[38] Y. I. Tien, K. H. Wei, *Macromolecules* **2001**, *34*, 9045.

[39] C. K. Kim, B. K. Kim, H. M. Jeong, *Colloid Polym. Sci.* **1991**, *269*, 895.

[40] T. K. Chen, Y. I. Tien, K. H. Wei, *Polymer* **2000**, *41*, 1345.

[41] D. S. Kim, J. T. Kim, W. B. Woo, *J. Appl. Polym. Sci.* **2005**, *96*, 1641.

[42] P. Ni, J. Li, J. Suo, S. Li, *J. Appl. Polym. Sci.* **2004**, *94*, 534.

[43] T. Takeichi, Y. Guo, *J. Appl. Polym. Sci.* **2003**, *90*, 4075.

[44] J. H. Chang, Y. U. An, *J. Polym. Sci. Part B: Polym. Phys.* **2002**, *40*, 670.

[45] W. J. Choi, S. H. Kim, Y. J. Kim, S. C. Kim, *Polymer* **2004**, *45*, 6045.

[46] H. R. Fischer, L. H. Gielgens, T. P. M. Koster, *Acta Polym* **1999**, *50*, 122.